Streptomyces alleviate abiotic stress in plant by producing pteridic acids

Zhijie Yang[1], Emil Strøbech[1], Yijun Qiao[1], Naga Charan Konakall[2], Pernille Harris[3], Gundela Peschel[4], Miriam Agler-Rosenbaum[4], Tilmann Weber[5], Erik Andreasson[2], Ling Ding[1,*]

[1] Department of Biotechnology and Biomedicine, Technical University of Denmark, Søltofts Plads, Building 221, 2800 Kgs. Lyngby, Denmark.

[2] Department of Plant Protection Biology, Swedish University of Agricultural Sciences, Sundsvägen 14, SE-230 53, Alnarp, Sweden.

[3] Department of Chemistry, Technical University of Denmark, Søltofts Plads, Building 206, 2800 Kgs. Lyngby, Denmark.

[4] Leibniz Institute for Natural Product Research and Infection Biology - Hans Knöll Institute (HKI), Beutenbergstr. 11a, 07745 Jena, Germany.

[5] Novo Nordisk Foundation Center for Biosustainability, Technical University of Denmark, Kemitorvet, Building 220, 2800 Kgs. Lyngby, Denmark.

*Corresponding author: Ling Ding lidi@dtu.dk

Abstract

Soil microbiota can confer fitness advantages to plants and increase crop resilience to drought and other abiotic stressors. However, there is little evidence on the mechanisms correlating a microbial trait with plant abiotic stress tolerance. Here, we report that *Streptomyces* effectively alleviates the drought and salinity stress by producing spiroketal polyketide pteridic acid H (**1**) and its isomer F (**2**), both of which promote root growth in *Arabidopsis* at a concentration of 1.3 nM under abiotic stress. Pteridic acids induce stress response genes expression in salinity-stressed *Arabidopsis* seedlings. The bifunctional biosynthetic gene cluster of pteridic acids and antimicrobial elaiophylin is confirmed in vivo and mainly disseminated by vertical transmission which is geographically distributed in various environments. This discovery reveals a perspective for understanding plant-*Streptomyces* interactions and provides a promising approach for utilising beneficial *Streptomyces* and their secondary metabolites in agriculture to mitigate the detrimental effects of climate change.

Introduction

According to the Food and Agriculture Organization of the United Nations, climate change generates considerable uncertainty about future water availability in many regions. Increased water scarcity under climate change will present a major challenge for climate adaptation, while sea-level rise will affect the salinity of surface and groundwater in coastal areas. Stress caused by climate change has led to increased agricultural losses and threatened global food security.[1,2] Drought is considered the most damaging environmental stress, which directly affects the entire growth period of plant seeds from germination to final fruiting.[3] Drought stress can lead to increased plant osmotic regulators, the inhibition of photosynthesis, and the change of plant endogenous hormone content.[4-6] Drought stress also induces reactive oxygen species (ROS), such as superoxide radicals, hydrogen peroxide, and hydroxyl radicals, leading to oxidative stress.[7] At high concentrations, ROS can cause damage at various tissue levels, for example, triggering lipid peroxidation and membrane degradation in plants.[8,9] Crop loss due to soil salinisation is another increasing threat to agriculture worldwide, which is more severe in agricultural land in coastal and arid regions.[10] Irrigation with saline water, low precipitation, and high evapotranspiration are key factors of the rapid salinisation of agricultural land.[11] These abiotic stresses of drought and salinity have brought unprecedented challenges to the development of crop farming. Compared to the heavy use of chemical fertilisers, the use of plant growth-promoting bacteria to improve plant growth under drought and salinity environments is more sustainable and gaining more attention.[12,13]

Soil microbial communities are critical to plant health and their resistance to both biotic and abiotic stressors, such as pathogens, drought, salinity, and heavy metal pollution.[14] A few studies have demonstrated that many beneficial soil bacteria harbour plant growth-promoting activities, *e.g.* by helping plants with disease suppression,[15] nutrient acquisition,[16] phosphorus uptake[17] and nitrogen fixations.[18] Beneficial root microbiota also regulates biosynthetic pathways in the plant itself, leading to differential alterations in the plant metabolome in response to stresses.[19] *Streptomyces* are Gram-positive filamentous bacteria, widely distributed in soil and marine environments. While they have long been considered the richest source of bioactive secondary metabolites,[20] *Streptomyces* have recently drawn attention as a class of plant growth-promoting bacteria that help plants respond to adversity stress.[21] The growing evidence showed that *Streptomyces* can promote plant growth or tolerance to stressors in direct or indirect ways, by secreting plant growth regulator auxin (indole-3-acetic acid, IAA) and siderophores, inducing systemic resistance in plants, and regulating the rhizosphere microbiome via producing antibacterial compounds or signalling molecules.[22-24] Notably, the commercial product Actinovate® and Mycostop® are two *Streptomyces*-based formulations that

have been widely used to suppress a wide range of diseases in a variety of crop groups as a biological fungicide/bactericide for the long term. Recently, the enrichment of *Streptomyces* has also been shown to play a subsequent role in the drought/salt tolerance of plants.[25] Despite the widespread claims of efficacy of inoculation of plant growth-promoting *Streptomyces*, the molecular basis of the growth-promoting effects and the key role of secondary/specialised metabolites in this process are largely unknown.

Here, we report that *Streptomyces iranensis* HM 35 has profound beneficial effects on helping barley alleviate osmotic, drought and salinity stress. The active components were identified as a bioactive spiroketal polyketide pteridic acids H (**1**) and its isomer F (**2**) through large-scale fermentation and bioactivity-directed purification followed by NMR, MS, and X-ray crystallography. The abiotic stress mitigating effect of pteridic acids H and F have been confirmed on the model plant *Arabidopsis thaliana,* where it effectively reversed both drought and salinity stress as phytohormone-like small biomolecules at concentrations as low as 0.5 ng mL^{-1} (1.3 nM). Moreover, the Biosynthetic Gene Cluster (BGC) of pteridic acids (*pta*) was identified and analysed in silico and functionally confirmed by in vivo CRISPR-based genome editing. We have furthermore conducted a survey of 81 potential producers of pteridic acids, which are widely distributed around the world. Phylogenetic and comparative genomic analysis of *pta*-containing *Streptomyces* suggested that these strains have evolutionary convergence in disseminating *pta* BGC through main vertical transmission and occasional horizontal gene transfer. In summary, we reveal a strategy of *Streptomyces* to secret plant growth regulators that help plants cope with abiotic stresses, which is a promising alternative solution for plant development and crop yields under the current climate change-induced environmental stresses.

Results

Abiotic Stress-Mitigating Activities Exhibited by *S. iranensis*. The promotion of barley growth induced by *S. iranensis* was tested under multiple abiotic stresses including osmotic, salinity and drought. The osmotic stress experiment was simulated using soils supplemented with 20% (w/v) PEG-6000 by transiently reducing the water potential (Ψ_W) of the plant. We found that the *S. iranensis* played a significant role in alleviating osmotic stress in barley seedlings. The treated seedlings showed a significant increase in height, fresh weight, and dry weight compared to the control group without any extra treatment (Fig. 1a). The culture broth of *S. iranensis* also showed considerable activity for the growth of barley in alleviating salinity stress mediated by 100 mM NaCl (Fig. 1b), while *S. iranensis* was not significantly enriched in the soil around the roots of barley seedlings (Supplementary Fig. 1). Additionally, based on the analysis of barley seedling phenotypes, the treatment with *S.*

iranensis resulted in a significant improvement in plant growth recovery from drought stress (Fig. 1c). Surprisingly, *S. iranensis* promoted the growth of barley seedlings even in non-stress growth condition and thus indicate that *S. iranensis* may have potential for use in biocontrol (Supplementary Fig. 2).

Genomic and metabolomic profiles of *S. iranensis*. To reveal the potential bioactive components, we first annotated BGCs responsible for the biosynthesis of secondary metabolites in *S. iranensis* using antiSMASH 6.0.[26] Genome sequence analysis of *S. iranensis* revealed the presence of 50 putative secondary metabolites BGCs with a variety of biosynthetic categories (Supplementary Tab. 1). The clusters 4, 7, 8, 9, 24, 32, 36 and 41 were annotated to have greater than 85% similarity with BGCs responsible for the biosynthesis of coelichelin, azalomycin, nigericin, elaiophylin, desferrioxamin, ectoine, rapamycin and hygrocin, respectively. Their corresponding products were also detected and identified through High-resolution Liquid Chromatography-tandem Mass Spectrometry (HR-LC-MS/MS) as well as Global Natural Products Social (GNPS) molecular networking (Fig. 1d, Supplementary Fig. 3).[27] However, there are still a number of metabolites of *S. iranensis* are still unknown. Since none of the previously identified compounds have been associated with mitigating abiotic stress in plants, we were prompted to expand the fermentation process and identify the potential bioactive compounds.

Characterisation of the bioactive compound pteridic acid. To uncover the bioactive components, fermentation of *S. iranensis* was scaled up to 175 litres and the culture broth was subjected to separation through open-column chromatography on Amberchrom CG161Me resin, silica gel, and Sephadex LH-20. Bioactivity-guided fractionation led to the isolation of bioactive compound **1** (15.0 mg) together with another structurally related compound **2** (4.0 mg) (Fig. 1e).

The bioactive component compound **1** was isolated as a white solid. Its formula of $C_{21}H_{34}O_6$ was deduced by *m/z* 383.2439 $[M+H]^+$ (calculated for 383.2428, Δ 2.84 ppm). The ^{1}H NMR spectrum exhibited signals for four olefinic protons (δ 7.33, 6.26, 6.13, 5.90) corresponding to two conjugated double bonds, four oxygen-bearing methines (δ 3.85, 3.69, 3.59, 3.43), five methyls, and other aliphatic protons. The ^{13}C NMR spectrum indicated the presence of one carbonyl group (δ 168.7) and one oxygen-bearing quaternary carbon (δ 103.2, C-11). The COSY spectrum established two partial substructures, which could be connected via a spiral function by analysing HSQC and HMBC correlations (Supplementary Fig. 4-11). Compound **1** was crystallised in methanol solution, and the structure was determined via X-ray crystallography (Supplementary Fig. 12). Therefore, compound **1** was identified as a new *Streptomyces*-derived natural product named pteridic acid H.

Compound **2**, a white solid, is an isomer of **1** since MS deduced the same molecular formula of $C_{21}H_{34}O_6$. The ^{1}H NMR spectrum exhibited signals for four olefinic protons (δ 7.16, 6.25, 6.07, 5.97)

corresponding to two conjugated double bonds, four oxygen-bearing methines (δ 3.88, 3.66, 3.56, 3.32), five methyls, and other aliphatic protons. The ^{13}C NMR spectrum indicated the presence of one carbonyl group (δ 170.2) and one oxygen-bearing quaternary carbon (δ 103.2, C-11). HSQC and HMBC correlations confirmed a spiroketal skeleton. NOESY spectrum confirmed its relative configurations, where correlations between H-21 and H-13 and H-15, H-7 and H-12a, and H6, H-10, and Me-18 were observed. The key NOESY correlations between H-7 and H-12a revealed a different spiroketal structure than **1** (Supplementary Fig. 11, 13-20). This can be reflected by the relative up-field NMR data for C-12 (δ 33.8 vs δ 37.5 in **1**). Compound **2** was identified as pteridic acid F, previously isolated from *Streptomyces pseudoverticillus* YN17707 and a marine-derived *Streptomyces* sp. SCSGAA 0027.[28,29]

Abiotic stress mitigation of pteridic acids *in planta*. Initially, we tested the effects of different concentrations of pteridic acids H and F on *Arabidopsis* growth in the absence of abiotic stress. A concentration of 0.5 ng ml^{-1} of both pteridic acids H and F was found to significantly promote the growth of *Arabidopsis* seedlings (Supplementary Fig. 21). Under drought stress, pteridic acid H at a concentration of 0.5 ng mL^{-1} increased the root length and fresh weight of *Arabidopsis* seedlings by 54.5% and 89%, respectively, and its activity was significantly better than the IAA and ABA at the same molar concentration (Fig. 2a, 2c). The treatment of pteridic acid F also showed great activity in alleviating drought stress, and the root length and fresh weight were increased by 30.5% and 56.7%, respectively (Fig. 2c). Pteridic acids H and F also showed significant activity in alleviating NaCl-mediated salinity stress (Fig. 2b. 2d). Compared to the non-treated groups, the treatment of 0.5 ng mL^{-1} pteridic acids H and F increased root length of *Arabidopsis* seedlings by 74.0% and 61.8%, as well as fresh weight by 126.2% and 110.9%, respectively (Fig. 2d).

To gain insights into how plants respond to pteridic acids, we performed quantitative real-time PCR (qRT-PCR) analysis to measure the expression levels of stress response genes TONOPLAST INTRINSIC PROTEIN 2;3 (TIP2;3) and SALT OVERLY SENSITIVE 1 (SOS1) in *Arabidopsis* seedlings, induced by pteridic acids H and F under salinity stress. Compared to the control, the relative expression level of TIP2;3 was significantly increased following both 1-hour and 24-hour treatments, while the transcript levels of SOS1 was down-regulated at 1-hour while up- regulated at 24-hour (Fig. 2e). This result indicated that pteridic acids H and F regulated the TIP2;3 and SOS1 to activate stress-resistance responses in plants.

A previous study suggested that pteridic acids A and B might have a plant growth-promoting effect like IAA and could stimulate the formation of adventitious roots in kidney beans.[28] However, we observed that pteridic acids H and F displayed the different IAA-induced phenotypes. Pteridic acids

did not exhibit the function to significantly promote lateral root growth of *Arabidopsis* seedlings like IAA (Fig. 2f, 2g).[30] We also found that pteridic acids were also not capable of promoting the formation of adventitious roots in kidney beans, as shown in Supplementary Fig. S22. Except for drought and salinity stress, we also tested the $CuSO_4$-mediated heavy metal stress alleviation activity of pteridic acids in mung beans. The results showed that the 1 ng mL^{-1} pteridic acid H was effective as ABA in helping mung beans to relieve heavy metal stress (Supplementary Fig. S23). In conclusion, pteridic acids H and F are widely applicable potent plant growth regulators produced by *Streptomyces* to assist plants in coping with different abiotic stress.

Biosynthesis of pteridic acids. The retro-biosynthesis analysis indicated that pteridic acids could derive from a modular type I polyketide synthase. A putative *pta* BGC was identified in the whole genome sequence of S. *iranensis*, which shows 87% antiSMASH similarity to the BGC of elaiophylin (BGC0000053 in MiBiG database).[31] The *pta* BGC spans approximately 56 kb and encodes 20 individual biosynthetic genes responsible for the biosynthesis of core polyketide backbones, precursor, glycosylated substituents, transporters and regulators (Supplementary Tab. 2). The five consecutive Type I polyketide synthase (PKS) encoding genes within the *pta* BGC consist of one loading module and seven extender modules, which are sequentially extended to form a linear polyketide chain by ketosynthase (KS) domain, acyltransferase (AT) domain, acyl carrier protein (ACP), with additional ketoreductase (KR), dehydratase (DH), and enoyl reductase (ER) domains. The substrate specificity predictions for individual AT domains fit well with the structure of pteridic acids (Supplementary Tab. 3). The last "Asn" residue is absent in the conserved Lys-Ser-Tyr-Asn tetrad of the KR domain in module 3 (PtaB), which is predicted to be inactive (Supplementary Fig. 24). This is consistent with the nonreduced carbonyl group on the α-carbon in module 3. The first DH domain in module 1 is inactive since it does not have a conserved active motif LxxHxxGxxxxP (Supplementary Fig. 25). Following the thioesterase-mediated release of the polyketide chain, the 6,6-spiroketal core structure is likely formed by spontaneous spiroketalisation of the carbonyl group on C11 and the two hydroxyl groups on C17 and C25. Following a loss of H_2O, two differentially oriented spirocyclic rings were formed to yield pteridic acids F and H (Fig. 3a). Remarkably, pteridic acid H showed molecular instability under extreme conditions. In the water solution with high temperature (65°C) or acidity (pH = 3), pteridic acid H is transformed into pteridic acid F (Supplementary Fig. 26). A similar spontaneous transformation from (*S*) to (*R*) chirality at the centre of the spiroketal ring was also observed in 6,6-spiroketal avermectin.[32]

CRISPR base editing in *S. iranensis*. To validate the *in silico* prediction of BGC, we utilized the efficient base editing tool CRISPR-cBEST to further confirm *pta* BGC.[33] As a non-model *Streptomyces* strain, *S. iranensis* is hard to genetically manipulate through intergeneric conjugation.[34] Therefore, the conjugation process was systematically optimised in this study (Supplementary Fig. 27). The core polyketide synthase *ptaA* was targeted and inactivated by converting a TGG (Trp) codon at position 916 into the stop codon TAA using CRISPR base editing. The editing event was confirmed by PCR amplification and Sanger sequencing of the editing site (Fig. 3c). As expected, the production of both pteridic acids and elaiophylin was abolished in *S. iranensis*/Δ*ptaA* (Fig. 3c). Plant experiments showed that the treatment of *S. iranensis*/Δ*ptaA* fermentation suspension led to the abolishment of the abiotic stress mitigating effects (Fig. 1a, 1b, 1c). To further confirm *pta* gene cluster, a bacterial artificial chromosome (BAC) library of *S. iranensis* was constructed. BAC-based cross-complementation of the *ptaA* in *S. iranensis*/Δ*ptaA* restored the production of pteridic acids and elaiophylin (Supplementary Fig. 28).

Interestingly, based on isotope-labelled precursor feeding and partial cosmid sequencing-based bioinformatics prediction, this BGC has long been inferred to be responsible for the biosynthesis of the antibacterial elaiophylin.[35,36] In 2015, Zhou et al. reported that thioesterase in the last module catalyse the formation of symmetrical macrodiolide using two units of linear elaiophylin monomeric seco acid (Fig. 3b).[37] To confirm whether the biosynthesis of pteridic acids is also thioesterase-dependent, site-specific mutations of residues Met-Glu-Asp to Ile-Lys-Met were introduced into the active sites of the TE domain *in vivo* (Supplementary Fig. S29).[38] The HR-LC-MS/MS analysis showed that the mutant strain (M2089I+E2090K+D2091M) no longer produced pteridic acids and elaiophylin (Fig. 3d). Hence, we provide additional evidence via in vivo inactivation and site-directed mutagenesis. Co-production of the plant growth-regulating pteridic acids and the antimicrobial elaiophylin through a shared BGC is intriguing and points to possible joint efforts in helping plants cope with biotic and abiotic stress.

Geographical distribution of pteridic acid producers. We surveyed available gene cluster family (GCF) data for all bacteria in the BiG-FAM database.[39] We found that *pta* BGC (GCF_02696) is strictly restricted to the *Streptomyces* genus. In addition, a total of 55 BGCs with high similarity to the *pta* BGC were detected by BiG-SCAPE,[40] among a total of 9,386 type I polyketides BGCs in 1,965 *Streptomyces* from the NCBI assembly database. Through literature supplementation and data dereplication of other reported producers without sequence information, at least 81 *Streptomyces* are known to produce pteridic acids/elaiophylin or have specific *pta* BGC up to date (Supplementary Tab. 4). Based on the known sampling information, the *pta*-containing *Streptomyces* display a variety of

geographic distribution and biological origins (Fig. 4). We selected two available *Streptomyces* strains (*Streptomyces violaceusniger* Tu 4113 and *Streptomyces rapamycinicus* NRRL 5491) to test the potential plant growth-promoting activity of these potential pteridic acid producers. The HR-LC-MS/MS analysis of both culture broths revealed that they shared similar metabolite profiles, and both produced pteridic acids H and F (Supplementary Fig. 30). Treatment with both culture broths on barley seedlings also exhibited significant plant growth-promoting activities under osmotic, salinity and drought stress (Fig. 4b, 4c and 4d). This evidence suggests that this class of *Streptomyces* and its specific secondary metabolite pteridic acids have unique ecological significance involved in plant abiotic stress resistance.

Phylogeny and evolution of *pta* BGC. To explore the evolutionary clues of pteridic acid producers, 16S rRNA genes were initially used to assess the relatedness of the collected 34 potential producers of pteridic acids with other *Streptomyces* strains that do not contain *pta* BGC. (Fig. 5a; Supplementary Fig. 31). The results revealed that, except for *Streptomyces albus* DSM 41398 and *Streptomyces* sp. GMR22, and other *pta*-containing *Streptomyces* strains cluster together and are distinct with divergent lineages. To further confirm this hypothesis, two high-resolution *Streptomyces* housekeeping genes, tryptophan synthase subunit beta (*trpB*) and RNA polymerase subunit beta (*rpoB*) were employed to analyse the phylogeny relationship among these strains.[41] Consequently, only *S. albus* DSM 41398 was classified in a distinct phylogenetic lineage among the *Streptomyces* strains containing *pta* BGC. The strict congruence among the clades of the housekeeping genes indicated dominant vertical transmission and potential horizontal gene transfer of the *pta* BGC in *Streptomyces*.

A total of 15 *pta*-containing *Streptomyces* with complete genome sequence information were selected to conduct the comparative genomics investigation. The genetic diversity in these *Streptomyces* strains was initially revealed using genome sequence similarity analysis. Except for *S. albus* DSM 41398 and *Streptomyces* sp. NA02950, we observed a high degree of similarity in the aligned region, as indicated by both the average nucleotide identity (ANI) and the alignment percentage (AP) among these strains (Supplementary Fig. 32). Genome synteny analysis revealed that partial genome rearrangements happened among strains even with high sequence similarities (Supplementary Fig. 33). Notably, the *pta* BGC in *S. albus* DSM 41398 (*pta-alb*) is located at the end of the chromosome, a high variable region in *Streptomyces*, suggesting its existence by accepting heterologous biosynthetic gene fragments. The nucleotide sequence alignment of *pta* BGC results showed that *pta-alb* is relatively complete, and the similarity of core genes is proportional to evolutionary relatedness (Fig. 5b). The metabolite profile of *S. albus* DSM 41398 also confirmed the integrity of the *pta-alb* by detecting the production of elaiophylin and pteridic acid H (Supplementary

Fig. 34). To further assess the biosynthesis diversity in remaining genetically related strains, we performed a BGCs similarity analysis (Supplementary Fig. 35, 36). The connections between their secondary metabolites, BGCs, revealed that these vertically inherited *Streptomyces* strains also harbour striking similarities. Combining phylogenetic and comparative genomics analysis, we expect that *S. albus* DSM 41398 is evolutionarily the most distinct member from other *pta*-containing *Streptomyces* strains and obtained the *pta* BGC via horizontal gene transfer. However, most *pta*-containing *Streptomyces* strains have vertically inherited *pta* and other gene clusters from their ancient ancestors that may be ecologically important and rarely studied.

Discussion

Drought and salinisation of soil are increasing globally, driving a reduction in crop yields that threatens food security. Plant growth-promoting bacteria is a class of beneficial microorganisms that positively interact with the plant to confer environmental stresses.[42,43] Although some *Streptomyces* species have been reported to have plant growth-promoting activity, the molecules mediating such positive effects are poorly understood. Deciphering the molecular mechanism is key to understanding the complex plant microbiota interaction. In this study, we present an example of *S. iranensis* secreting a family of secondary metabolites, pteridic acids, to assist plants to cope with abiotic stresses like osmotic, salinity and drought. Pteridic acids H and F were chemically isolated, structurally characterised and functional validated as plant-beneficial molecules.

Plants respond to the harsh environment by changing their physiological processes for better survival.[44] Salt and drought stress signal transduction consists of ionic and osmotic homeostasis signaling pathways, detoxification (i.e., damage control and repair) response pathways, and pathways for growth regulation.[45] Aquaporins are membrane channels that facilitate the uptake of soil water and mediate the regulation of root hydraulic conductivity in response to a large variety of environmental stresses. [46] TIPs represent one family of aquaporins, and they are involved in regulating water flow in response to osmotic challenges like drought or salinity for a plant cell.[47] In our study, treatment of pteridic acids H and F resulted in a 2.1-fold and 2-fold increase in TIP2;3 transcripts at 1-hour and a 2.1-fold and 2.9-fold increase at 24-hour, respectively (Fig. 2e). SOS1 is a plasma membrane Na^+/H^+ antiporter, which is important for plant to alleviate salinity stress.[48] In response to the ionic toxicity triggered by salt stress, plants rely on the Salt Overly Sensitive (SOS) pathway to transport excessive Na^+ from the cytoplasm to the apoplast, thus ensuring endogenous ionic homeostasis.[49] The overexpression of SOS1 could significantly increase the salt tolerance of *Arabidopsis* plants.[50] We noticed that the relative expression of SOS1 was significantly enhanced after the 24-hour treatment of pteridic acids, which preliminary revealed the molecular basis that endows it with stress resistance.

However, the exact mode of action of pteridic acids remains to be further investigated by for example genome-wide transcriptomics screening for pteridic acids insensitive mutant plants.

Horizontal gene transfer is an integral driver of BGC evolution, revealing the independent processes of species phylogeny and BGCs distribution.[51] However, vertical inheritance also influences BGCs evolutionary dynamics, evident from BGCs conservation among closely related strains.[52] We found that the *pta* BGC in *Streptomyces* are widely dispersed geographically and mainly inherited through vertical gene transmission. Some of these strains have also been described to have remarkable biocontrol capabilities. For example, *Streptomyces* sp. AgN23 activates *Arabidopsis* defence responses to fungal pathogen infection by secreting plant elicitors,[53] *Streptomyces rhizosphaericus* 0250 and *Streptomyces* sp. 5-10 displayed significant biocontrol potential to fusarium wilt of bitter gourd.[54,55] The family of *pta*-containing *Streptomyces* was also previously described as a specific phylogenetic lineage with the highest BGC abundance and largest genome size across diverse *Streptomyces-type* strains.[56] Although the biosynthetic diversity of these *Streptomyces* is likely due to horizontal transfer events that occurred relatively recently in their evolutionary history instead of genetic diversification through a vertical transfer of BGCs. The multiple Type I PKSs presenting among these strains are highly conserved based on genetic similarity network analysis. There is currently some evidence supporting potential complex cross-BGC regulation in this class of *Streptomyces* strains. Jiang et al. demonstrated that a TetR family transcriptional regulator, GdmRIII, controls the biosynthesis of geldanamycin and elaiophylin meanwhile, in *Streptomyces autolyticus* CGMCC 0516.[57] Recently, He et al. found that the rapamycin BGC-situated LAL family regulator RapH co-ordinately regulated the biosynthesis of both rapamycin and elaiophylin in *S. rapamycinicus* NRRL 5491.[58] Although these reports correspond to cross-regulation between evolutionarily conserved BGCs, more details of these communications need to be investigated.

In conclusion, pteridic acids are secondary metabolites produced by *Streptomyces* enhancing plant resistance to abiotic stress. This is a useful illustration of the bacterial metabolite-mediated alteration of plants in response to environmental stress. It will open avenues for utilising *Streptomyces* to rewild plant microbiomes and improve plant abiotic stress resistance to tackle climate change.[59]

Methods

Strains, plasmids, and cultivation. All strains and plasmids used in this study were listed in Supplementary Tab. 5. All *Streptomyces* strains were obtained from the German Collection of Microorganisms and Cell Cultures GmbH (DSMZ, Germany). All *Escherichia coli* strains were grown in liquid/solid LB medium (5.0 g L^{-1} yeast extract, 10.0 g L^{-1} peptone, 10.0 g L^{-1} NaCl) at 37°C. All *Streptomyces* strains were grown on SFM medium (20.0 g L^{-1} mannitol, 20.0 g L^{-1} soya flour, 20.0 g

L^{-1} agar), and the SFM medium with the addition of 120 mM calcium chloride solution was used for the step of conjugation at 28°C. The ISP2 medium (4.0 g L^{-1} yeast extract, 10.0 g L^{-1} malt extract, 4.0 g L^{-1} dextrose, and 1.0 L distilled water) was used for liquid fermentation of all *Streptomyces* strains used in plant assay and metabolomics analysis. Appropriate antibiotics were supplemented with the following working concentrations: apramycin (50 µg mL^{-1}), chloramphenicol (25 µg mL^{-1}), and kanamycin (50 µg mL^{-1}). All chemicals utilized in this study were from Sigma-Aldrich, USA.

Metabolomics analyses. High performance liquid chromatography was carried out on the Agilent Infinity 1290 UHPLC system (Agilent Technologies, USA). The 250 × 2.1 mm i.d., 2.7 µm, Poroshell 120 Phenyl Hexyl column (Agilent Technologies, USA) was used for separation. The 2-µL samples were eluted at a flow rate of 0.35 mL min^{-1} using a linear gradient from 10% acetonitrile in Milli-Q water buffered with 20 mM formic acid increasing to 100% in 15 min. Each starting condition was held for 3 min before the next run. Mass spectrometry detection was performed on an Agilent 6545 QTOF MS equipped with Agilent Dual Jet Stream electrospray ion source (ESI) with a drying gas temperature of 160°C, a gas flow of 13 L min^{-1}, sheath gas temperature of 300°C, and flow of 16 L min^{-1}. The capillary voltage was set to 4000 V and the nozzle voltage to 500 V in positive mode. MS spectra were recorded as centroid data at an m/z of 100-1700, and auto MS/HRMS fragmentation was performed at three collision energies (10, 20, and 40 eV) on the three most intense precursor peaks per program. Data were analysed with MassHunter software (Agilent Technologies, USA) and compared with known compounds and crude extract spectral libraries stored in the GNPS platform.[45] The precursor and fragment ion mass tolerance were set as 0.1 Da and 0.02 Da, respectively. In addition, the minpairs cos was set as 0.65, and the minimum matched fragment ions were set as 6.0. The metabolites profile of wild-type *S. iranensis* was visualised by MS-Dial 4.9.2.[60]

Large-scale fermentation and isolation. *S. iranensis* was cultivated in medium 2 (3.0 g L^{-1} $CaCl_2{\cdot}2H_2O$, 1.0 g L^{-1} citric acid/Fe III, 0.2 g L^{-1} $MnSO_4{\cdot}H_2O$, 0.1 g L^{-1} $ZnCl_2$, 0.025 g L^{-1} $CuSO_4{\cdot}5H_2O$, 0.02 g L^{-1} $Na_2B_4O_2{\cdot}10H_2O$, 0.01 g L^{-1} $NaMoO_4{\cdot}2H_2O$, and 20.0 g L^{-1} oatmeal in 1.0 L distilled water), at 175 L filling volume in a 300 L fermentation vessel (Sartorius, Germany). The fermentation was carried out for 6 days with aeration of 25-50 L min^{-1}, stirring at 200 rpm with a temperature of 28°C and at a pH range of 5.4-6.4. The fermentation broth was separated, filtered, and loaded onto an Amberchrom CG161Me resin LC column (200 × 20 cm, 6 L). Elution with a linear gradient of H_2O-MeOH (from 30% to 100% v/v, flow rate 0.5 L min^{-1}, in 58 min) afforded seven fractions (A-G). Fraction G was firstly fractionated by silica gel chromatography with a CH_2Cl_2/CH_3OH gradient to yield 16 fractions, F01-F16. F07 was separated by a Sephadex LH-20

(MeOH) column and twelve sub-fractions F07a-l were obtained. From F07e, **1** (15.0 mg) and **2** (4.0 mg) were obtained by repeated HPLC RP-C_{18} (CH_3CN/H_2O as gradient).

Pteridic acid H (**1**): white solid; $[\alpha]_D^{20}$ 81 (0.32 mg/mL, CH_3OH), ^{1}H NMR (800 MHz, MeOD): 7.33 (dd, 15.4 Hz, 11.1 Hz, 1H), 6.26 (dd, 15.2 Hz, 10.8 Hz, 1H), 6.13 (dd, 15.3 Hz, 8.8 Hz, 1H), 5.90 (d, 15.4 Hz, 1H), 3.85 (dd, 10.2 Hz, 2.2 Hz, 1H), 3.69 (dd, 11.4 Hz, 4.9 Hz, 1H), 3.59 (m, 1H), 3.43 (m, 1H), 2.48 (m, 1H), 2.29 (dd, 14.9 Hz, 6.1 Hz, 1H), 2.01 (m, 1H), 1.64 (dd, 14.9 Hz, 1.9 Hz, 1H), 1.52 (m, 1H), 1.49 (m), 1.21 (d, 6.1 Hz, 3H), 1.01 (d, 6.8 Hz, 3H), 0.96 (d, 6.8 Hz, 3H), 0.93 (t, 7.3 Hz, 3H), 0.91 (d, 7.0 Hz, 3H); ^{13}CNMR (200 MHz, MeOD): 168.7, 151.0, 146.7, 129.6, 120.6, 103.2, 75.5, 72.8, 72.7, 70.3, 51.3, 42.2, 40.4, 37.5, 37.4, 24.8, 20.9, 16.0, 12.1, 11.1, 5.0; UV/vis (CH_3CN/H_2O) λ_{max} 262 nm; IR (ATR) ν_{max} 2967, 2934, 2879, 1712, 1642, 1600, 1458, 1410, 1383, 1300, 1266, 1223, 1187, 1142, 1109, 1058, 1002, 973 cm^{-1}; (+)-HR-ESI-MS (*m/z*) $[M+H]^+$ calcd for $C_{21}H_{35}O_6$, 383.2428; found, 383.2439. ^{1}H NMR and ^{13}C NMR see Supplementary Tab. 6.

Pteridic acid F (**2**): white solid; $[\alpha]_D^{20}$ -18 (10 mg/mL, CH_3OH), ^{1}H NMR (800 MHz, MeOD): 7.16 (dd, 15.1 Hz, 10.9 Hz, 1H), 6.25 (dd, 15.1 Hz, 10.9 Hz, 1H), 6.07 (dd, 15.1 Hz, 8.6 Hz, 1H), 5.97 (d, 15.1 Hz, 1H), 3.88 (m, 1H), 3.66 (td, 10.8 Hz, 4.3 Hz, 1H), 3.56 (dd, 11.5 Hz, 4.7 Hz, 1H), 3.32 (m, 1H), 2.49 (m, 1H), 2.19 (dd, 13.1 Hz, 4.3 Hz, 1H), 2.02 (m, 1H), 1.69 (m, 1H), 1.60 (m, 1H), 1.44 (m, 1H), 1.32 (dd, 13.2 Hz, 11.2 Hz, 1H), 1.14 (d, 6.2 Hz, 3H), 1.02 (m, 1H), 1.02 (d, 6.8 Hz, 3H), 0.95 (d, 6.9 Hz, 3H), 0.98 (d, 6.8 Hz, 3H), 1.60 (m, 1H), 1.44 (m, 1H), 0.82 (t, 7.6 Hz, 3H); ^{13}CNMR (200 MHz, MeOD): 170.2, 148.1, 143.4, 129,6, 122.9, 103.2, 77.7, 74.7, 69.8, 66.3, 52.2, 42.1, 40.5, 37.7, 33.8, 20.4, 19.7, 15.9, 12.7, 10.5, 5.3; UV/vis (CH_3CN/H_2O) λ_{max} 264 nm; IR (ATR) ν_{max} 2968, 2931, 2877, 1692, 1643, 1618, 1458, 1410, 1380, 1299, 1270, 1188, 1138, 1106, 1059, 1002, 973, 850 cm^{-1}; (+)-HR-ESI-MS (*m/z*): $[M+H]^+$ (calcd for $C_{21}H_{35}O_6$, 383.2428; found, 383.2433. ^{1}H NMR and ^{13}C NMR see Supplementary Tab. 7.

Structure identification. NMR spectra were recorded on an 800 MHz Bruker Avance III spectrometer equipped with a TCI CryoProbe using standard pulse sequences. NMR data were processed using MestReNova 11.0. UHPLC-HRMS was performed on an Agilent Infinity 1290 UHPLC system equipped with a diode array detector. UV-Vis spectra were recorded from 190 to 640 nm. Specific rotations were acquired using Perkin-Elmer 241 polarimeter. IR data were acquired on Bruker Alpha FTIR spectrometer using OPUS version 7.2. TLC analysis was performed on silica gel plates (Sil G/UV_{254}, 0.20 mm, Macherey-Nagel). The Biotage Isolera One Flash Chromatography system was used for flash chromatography and performed on silica gel 60 (Merck, 0.04–0.063 mm, 230–400 mesh ASTM). Sephadex LH-20 was from Pharmacia.

Crystal Structure Determination. X-ray data collection of **1** was performed on an Agilent Supernova Diffractometer using CuKα radiation. Data were processed and scaled using the CrysAlisPro software (Agilent Technologies, USA). The structure was solved using SHELXS and refined using SHELXL. Hydrogen atoms were included in ideal positions using riding coordinates. The absolute configuration was determined based on the Flack parameter. Crystal Data for **1**: $C_{21}H_{34}O_6$, Mr = 382.50, monoclinic, a = 8.4619(1) Å, b = 15.6161(2) Å, c = 8.4994(1) Å, α = 90.00°, β = 107.768(1)°, γ = 90.00°, V = 1069.55(2) Å3, T = 120(2) K, space group P21, Z = 2, μ(Cu Kα) = 0.698 mm–1, 17514 reflections collected, 4275 independent reflections (Rint = 0.0226, Rsigma = 0.0155). The final R1 values were 0.0249 (I > 2σ(I)). The final wR2 values were 0.0648 (I > 2σ(I)). The final R1 values were 0.0252 (all data). The final wR2 values were 0.0651 (all data). The goodness of fit on F2 was 1.057. The Flack parameter is 0.13(10).

Genetic manipulation. All primers used were synthesised by IDT (Integrated DNA Technologies, USA) and listed in Supplementary Tab. 8. Plasmids and genomic DNA purification, PCR and cloning were conducted according to standard procedures using manufacturer protocols. PCR was performed using OneTaq Quick-Load 2X Master Mix with Standard Buffer (New England Biolabs, USA). DNA assembly was done by using NEBuilder HiFi DNA Assembly Master Mix (New England Biolabs, USA). DNA digestion was performed with FastDigest restriction enzymes (Thermo Fisher Scientific, USA). NucleoSpin Gel and PCR Clean-up Kits (Macherey-Nagel, Germany) were used for DNA clean-up from PCR products and agarose gel extracts. One Shot Mach1 T1 Phage-Resistant Chemically Competent *E. coli* (Thermo Fisher Scientific, USA) was used for cloning. NucleoSpin Plasmid EasyPure Kit (Macherey-Nagel, Germany) was used for plasmid preparation. Sanger sequencing was carried out using a Mix2Seq Kit (Eurofins Scientific, Luxembourg). All DNA manipulation experiments were conducted according to standard procedures using manufacturer protocols.

Gene inactivation and site-directed mutagenesis. To use the pCRISPR-cBEST for base editing applications, an oligo was designed as Del-ptaA by the online tool CRISPy-web, and the pCRISPR-cBEST plasmid was linearised by *Nco*I. Mixing the linearised pCRISPR-cBEST plasmid and Del-ptaA with the NEBuilder HiFi DNA Assembly Master Mix (New England Biolabs, USA). The linearised pCRISPR-cBEST plasmid was then bridged by Del-ptaA, ending with the desired pCRISPR-cBEST/Δ*ptaA*. Chemically competent *E. coli* were transformed with the recombinant plasmid and confirmed via PCR amplification (program: 94°C for 30 s, followed by 30 cycles consisting of 94°C for 15 s; 54°C for 15 s; 68°C for 40 s, and 68°C for 2 min) and Sanger sequencing. The experimental

422 procedure for site-directed mutagenesis for the TE domain is the same as described above. The *E. coli-*
423 *Streptomyces* conjugation experiment was conducted according to the modified protocol in this study,
424 and the mutant *Streptomyces* strains were also confirmed by PCR and Sanger sequencing (Eurofins,
425 France).

426 **Construction of BAC and genetical complementation.** The BAC library of *S. iranensis* was
427 constructed using pESAC13-A from Bio S&T (Montreal, Canada). Based on a high-throughput
428 screening method (unpublished), we selected two BACs 1J23 and 6M10 that cross-cover the *ptaA* gene
429 (Supplementary Fig. 28). The selected BAC clones were further confirmed using four sets of primers,
430 including ID-1J23-right-F/R, ID-1J23-left-F/R, ID-6M10-right-F/R, and ID-6M10-left-F/R
431 (Supplementary Tab. 8). Subsequently, we introduced these two BAC clones 1J23 and 6M10 into *S.*
432 *iranensis*/Δ*ptaA* (remove the pCRISPR-cBEST/Δ*ptaA* to obtain antibiotics resistance free strain)
433 separately by conjugation. Exconjugants of mutants were further validated by apramycin-resistance
434 screening and PCR.

435 **Enrichment evaluation of *S. iranensis* in rhizosphere soil**. The *S. iranensis* (with the apramycin
436 resistance gene) spore suspension was well mixed with fully sterilised soil and was transferred to a
437 250 mL flask. The sterilised germinated barley seed was placed in the centre position of soil in flask
438 and grown at 24 ± 2°C, 8 h dark/16 h light in the growth chamber for 7 days. Samples were collected
439 from soil within 0.1 cm and 3 cm distance from the barley root, with a specification of 0.1 g soil per
440 sample. Then, these samples were transferred to sterilised 1.5 mL Eppendorf tubes and mixed with
441 500 μL sterilised H_2O. 200 μL of each sample was Spread evenly over the solid MS medium with the
442 addition of 50 μg mL^{-1} apramycin and grown at 28°C for 7 days. The number of *Streptomyces* colonies
443 grown on each plate were counted and statistically analysed.

444 ***Arabidopsis* growth assays.** *A. thaliana* ecotype Columbia (Col-0) was used to test the effects of
445 pteridic acid treatment under drought stress mediated by PEG-6000 (Duchefa Biochemie BV) and
446 salinity stress mediated by NaCl (Duchefa Biochemie BV). The modified Murashige & Skoog medium
447 (2.2 g L^{-1} Murashige & Skoog medium including B5 vitamins, 5.0 g L^{-1} of sucrose, 250 mg L^{-1} MES
448 monohydrate, 7.0 g L^{-1} agar, and adjusted pH to 5.7 with KOH) was used in this study. PEG-6000 (15%
449 w/v) was dissolved in water and filtered through 0.2-micron Sartorius Minisart™ Plus Syringe Filters
450 (Fisher Scientific). 50 mL of the filtered solution was overlaid onto the surface of solidified Murashige
451 & Skoog medium. The plates were left for 24 h to diffuse the PEG into the Murashige & Skoog medium.
452 NaCl was added to the medium to a final concentration of 80 mM for the salinity stress alleviation test.
453 The pure compound pteridic acids H and F (0.50 ng/mL), IAA (0.23 ng/mL), and ABA (0.34 ng/mL)

were mixed with different media to a final concentration of approximately 1.3 nM and poured into the plates. Seeds were surface sterilised by washing with 70% ethanol for 2 min, then in sterilisation solution (10% bleach) for 1 min by inverting the tubes, and finally washed five times with sterilised water. The seeds were stratified for 2 days at 4°C in the dark. Sterilised seeds were placed in Petri dishes (approx. 100 seeds per Petri dish) on Murashige & Skoog medium and grown for 3-4 days in the vertical position in a culture chamber at 22°C under standard long-day conditions (16/8 h light/dark photoperiod). After three days of growth, seedlings with similar root lengths (7-10 mm) were transferred to square plates containing Murashige & Skoog medium (control) or Murashige & Skoog medium supplemented with 15% (w/v) PEG-6000 or 80 mM NaCl. 16 seedlings were used per replicate for each treatment. The initial position of the plant root tip was marked with a marker. The plants were grown in the vertical position under standard long day conditions (22°C, 16/8h light/dark) for 8 days, and then each plate was scanned using Image Scanner. Primary and lateral root lengths and the total plant weight were then scored. The primary and lateral root length measurements were performed by analysing pictures with the Image J software. Fresh weight measurements were estimated using a precision balance. Whole 8-day-old plants grown in the medium were removed using forceps, dried in tissue paper, and then weighed using a precision balance.

Barley and mung bean growth assays. The pteridic acid *Streptomyces* producers were tested for their effects on barley cultivars Guld grown in soil. *S. iranensis* HM 35, *S. rapamycinicus* NRRL 5491, and *S. violaceusniger* Tu 4113 were cultivated in ISP2 medium for 7 days at 28˚C. 500 µL culture broth (ca. 3 x 10^9 CFU/mL) was added to 100 g sand soil and well mixed. Treated soils were infiltrated with Milli-Q water, 20% PEG-6000 solutions to simulate osmotic stress, and 100 mM NaCl solutions to simulate salinity stress in soil environments. To simulate drought stress during barley growth, the plant was initially watered for 7 days, then subjected to 7 days of drought stress, and finally allowed to recover with various treatments for another 7 days. Barley seeds were rinsed in distilled water and sterilised with 1% sodium hypochlorite for 15 min. They were then washed with distilled water and germinated in distilled water at 24°C for 2 days. Barley seeds were planted in each plastic pot (5cm x 5cm x 6cm, six seedlings per pot) supplemented with different treated soil and grown at 24 ± 2°C, 8 h dark/16 h light in the growth chamber for 7 days. Plant height (cm) was measured as the aerial part of the plant, and the fresh shoot weight (g) and fresh root weight (g) of each seedling were measured separately. Then, the seedlings were dried in the hot-air oven at 70°C for 6 h to obtain the dry shoot and dry root weights (g). For heavy metal stress experiment, mung beans were pre-germinated and placed on top of the modified Murashige & Skoog medium agar, supplemented with 10 mM CuSO4, with 1.0 ng/mL pure substances. All mung beans were grown in the dark at 24 ± 2°C for 4 days.

Kidney beans growth assays. The seeds of kidney beans (appr. 2 cm in length, from organic farming) were firstly sterilised successively with ethanol (70% v/v) and sodium hypochlorite (5% v/v), each for 2 min and then rinsed with sterile Milli-Q water (three times). The sterilised seeds were cultivated on modified Murashige & Skoog agar plates for 3-4 days. After germination, the seedlings (with 1.5-2 cm-long roots) were soaked in 10 mL aliquots of testing compounds (pteridic acids H and F, 1.0 ng/mL, dissolved in sterile Milli-Q water) in ultra-clear polypropylene containers (ø 34 mm, vol. 20 mL) with polyethylene caps. The control group was treated with 10 mL sterile Milli-Q water. For each treatment, three repetitions (containers) were used, and each repetition included four seedlings. After 24 h, the seeds were transferred into a cut square petri dish, put on the top layer of sandy soil, and then incubated vertically in a growth chamber (24/22°C, day/night cycle of 16/8 h, 50%, 60%, 70%, 100% of circulated wind velocity for 12 h, 2 h, 2h, 8h) for 7 days. Solutions of pteridic acids H and F (2 mL, 1.0 ng/mL for both) were added separately into corresponding containers, with sterile Milli-Q water as control, and an extra 8 mL of Milli-Q water was added to each petri dish every other day.

RNA extraction and quantitative real-time PCR. *Arabidopsis* seeds were sterilized, and seven to ten seeds were cultured in each well of a 24 well plate in 2 mL medium containing modified Murashige & Skoog and 30 mM sucrose with 16 hours light, at 24 °C in a controlled environment room. After 7 days, seedlings were washed in 20 mL modified Murashige & Skoog medium and then moved to 20 mL of fresh medium and cultured in 125ml E-flasks with 1 ng mL^{-1} of each pteridic acids H and F. Samples were collected at three Total RNA was extracted using RNeasy Plant Mini Kit (Qiagen, Germany) according to the manufacturer's instructions. Reverse transcription was performed using SuperScript™ III First-Strand Synthesis SuperMix for qRT-PCR (Invitrogen, USA). qRT-PCR was conducted on CFX96 Touch Real-Time PCR Detection System (Bio-Rad, USA) using Platinum SYBR Green qPCR SuperMix-UDG with ROX (Invitrogen, USA). The thermal cycling program consisted of an initial denaturation at 95 ℃ for 3 min, followed by 39 cycles of 95 ℃ for 15 s, 60 ℃ for 30 s. Three independent biological replicates were performed for each condition. TIP2;3 and SOS1 were used as target genes, and primers sequences were given in Supplementary Tab. 8. The expression level of target gene after treatments was calculated using the 2^ΔΔCt method, with ACT1 as the internal control.

Bioinformatics analyses. The identification and annotation of all BGCs of *Streptomyces* secondary metabolites were carried out with antiSMASH 6.0.[26] The threshold for similar BGCs was selected as greater than 45% sequence similarity. The BiG-FAM database and BiG-SCAPE software were used to identify the distribution of *pta* BGC in different bacteria and generate the *pta* family similarity

network.[39,40] A cut-off of 0.3 was used as a raw index similarity metric for the BiG-SCAPE analysis. The alignment of 15 *pta*-containing *Streptomyces* genome sequences was performed using the whole-genome alignment plugin of the CLC Genomics Workbench version 22.0.2 (Qiagen). The minimum initial seed length was 15 bp, and the minimum alignment block length was 100 bp. The networks of Big-SCAPE and GNPS analysis were visualised using Cytoscape 3.9. The phylogenetic analysis was conducted by the online multiple sequence alignment tool MAFFT and visualised by iTOL v5. [61,62]

Statistical analysis. Statistical significance was assessed by one-way ANOVA with post hoc Dunnett's multiple comparisons test, one-way ANOVA with Tukey test or t test (see each figure legends). All analyses were performed using GraphPad Prism version 9. *P*-values < 0.05 were considered significant. Asterisks indicate the level of statistical significance: $^{*}P < 0.05$, $^{**}P < 0.01$, $^{***}P < 0.001$, and $^{****}P < 0.0001$. For all relevant figures, source data and exact *P* values are provided in the Source Data file.

Data availability. The gene sequences used in this study were collected by searching National Center for Biotechnology Information (NCBI) or extracting from assembled genome sequences (attached in Supplementary information files). All genome sequences used in this study are publicly available on NCBI. The crystal structure was deposited at Cambridge Crystallographic Data Centre (https://www.ccdc.cam.ac.uk/) with CCDC deposition number 1984025. Metabolomics data in this study were deposited at https://massive.ucsd.edu with the identifier MSV000090745. Source data of each figure are provided with this paper.

References

1. Naylor, R., et al. A 20-year retrospective review of global aquaculture. *Nature* **591**, 551-563 (2021).
2. Wheeler, T. & von Braun, J. Climate change impacts on global food security. *Science* **341**, 508-513 (2013).
3. Zhang, H., Zhu, J., Gong, Z. & Zhu, J. Abiotic stress responses in plants. *Nat. Rev. Genet.* **23**, 104-119 (2022).
4. Kuromori, T., Fujita, M., Takahashi, F., Yamaguchi-Shinozaki, K. & Shinozaki, K. Inter-tissue and inter-organ signaling in drought stress response and phenotyping of drought tolerance. *Plant J.* **109**, 342-358 (2022).
5. Dos Santos, V., et al. Causes of reduced leaf-level photosynthesis during strong El Niño drought in a central Amazon forest. *Global Change Biol.* **24**, 4266-4279 (2018).
6. Waadt, R., et al. Plant hormone regulation of abiotic stress responses. *Nat. Rev. Mol. Cell Biol.* **23**, 680-694 (2022).

551 7. Kerchev, P. & Van Breusegem, F. Improving oxidative stress resilience in plants. *Plant J.* **109**, 359-
552 372 (2022).
553 8. Abid, M., et al. Physiological and biochemical changes during drought and recovery periods at
554 tillering and jointing stages in wheat (*Triticum aestivum* L.). *Sci. Rep.* **8**, 1-15 (2018).
555 9. Hasanuzzaman, M., et al. Regulation of ROS metabolism in plants under environmental stress: a
556 review of recent experimental evidence. *Int. J. Mol. Sci.* **21**, (2020).
557 10. Van Zelm, E., Zhang, Y. & Testerink, C. Salt tolerance mechanisms of plants. *Annu. Rev. Plant*
558 *Biol.* **71**, 403-433 (2020).
559 11. Corwin, D. Climate change impacts on soil salinity in agricultural areas. *Eur. J. Soil Sci.* **72**, 842-
560 862 (2021).
561 12. Hong, Y., Zhou, Q., Hao, Y. & Huang, A. C. Crafting the plant root metabolome for improved
562 microbe-assisted stress resilience. *New Phytol.* **234**, 1945-1950 (2022).
563 13. De Vries, F., Griffiths, R., Knight, C., Nicolitch, O. & Williams, A. Harnessing rhizosphere
564 microbiomes for drought-resilient crop production. *Science* **368**, 270-274 (2020).
565 14. Arif, I., Batool, M. & Schenk, P. Plant microbiome engineering: expected benefits for improved
566 crop growth and resilience. *Trends Biotechnol.* **38**, 1385-1396 (2020).
567 15. Berlanga-Clavero, M., et al. *Bacillus subtilis* biofilm matrix components target seed oil bodies to
568 promote growth and anti-fungal resistance in melon. *Nat. Microbiol.* **7**, 1-15 (2022).
569 16. Das, P., et al. Plant-soil-microbes: A tripartite interaction for nutrient acquisition and better plant
570 growth for sustainable agricultural practices. *Environ. Res.* **214**, 113821 (2022).
571 17. Hiruma, K., et al. Root endophyte *Colletotrichum tofieldiae* confers plant fitness benefits that are
572 phosphate status dependent. *Cell* **165**, 464-474 (2016).
573 18. Henneron, L., Kardol, P., Wardle, D., Cros, C. & Fontaine, S. Rhizosphere control of soil nitrogen
574 cycling: a key component of plant economic strategies. *New Phytol.* **228**, 1269-1282 (2020).
575 19. Etalo, D., Jeon, J. & Raaijmakers, J. Modulation of plant chemistry by beneficial root microbiota.
576 *Nat. Prod. Rep.* **35**, 398-409 (2018).
577 20. Quinn, G., Banat, A., Abdelhameed, A. & Banat, I. *Streptomyces* from traditional medicine: sources
578 of new innovations in antibiotic discovery. *J. Med. Microbiol.* **69**, 1040-1048 (2020).
579 21. Viaene, T., Langendries, S., Beirinckx, S., Maes, M. & Goormachtig, S. *Streptomyces* as a plant's
580 best friend? *FEMS Microbiol. Ecol.* **92**, (2016).
581 22. Myo, E., et al. Indole-3-acetic acid production by *Streptomyces fradiae* NKZ-259 and its
582 formulation to enhance plant growth. *BMC Microbiol.* **19**, 1-14 (2019).
583 23. Sadeghi, A., et al. Plant growth promoting activity of an auxin and siderophore producing isolate
584 of *Streptomyces* under saline soil conditions. *World J. Microbiol. Biotechnol.* **28**, 1503-1509 (2012).

585 24. Singh, S. & Gaur, R. Endophytic *Streptomyces* spp. underscore induction of defense regulatory
586 genes and confers resistance against *Sclerotium rolfsii* in chickpea. *Biol. Control* **104**, 44-56 (2017).
587 25. Fitzpatrick, C., et al. Assembly and ecological function of the root microbiome across angiosperm
588 plant species. *Proc. Natl. Acad. Sci. U. S. A.* **115**, E1157-E1165 (2018).
589 26. Blin, K., et al. antiSMASH 6.0: improving cluster detection and comparison capabilities. *Nucleic*
590 *Acids Res.* **49**, W29-W35 (2021).
591 27. Wang, M., et al. Sharing and community curation of mass spectrometry data with Global Natural
592 Products Social Molecular Networking. *Nat. Biotechnol.* **34**, 828-837 (2016).
593 28. Igarashi, Y., Iida, T., Yoshida, R. & Furumai, T. Pteridic acids A and B, novel plant growth
594 promoters with auxin-like activity from *Streptomyces hygroscopicus* TP-A0451. *J. Antibiot.* **55**, 764-
595 767 (2002).
596 29. Nong, X., Wei, X. & Qi, S. Pteridic acids C-G spirocyclic polyketides from the marine-derived
597 *Streptomyces* sp. SCSGAA 0027. *J. Antibiot.* **70**, 1047-1052 (2017).
598 30. Lavenus, J., et al. Lateral root development in *Arabidopsis*: fifty shades of auxin. *Trends Plant Sci.*
599 **18**, 455-463 (2013).
600 31. Kautsar, S., et al. MIBiG 2.0: a repository for biosynthetic gene clusters of known function. *Nucleic*
601 *Acids Res.* **48**, D454-D458 (2020).
602 32. Sun, P., et al. Spiroketal formation and modification in avermectin biosynthesis involves a dual
603 activity of AveC. *J. Am. Chem. Soc.* **135**, 1540-1548 (2013).
604 33. Tong, Y., et al. Highly efficient DSB-free base editing for streptomycetes with CRISPR-BEST.
605 *Proc. Natl. Acad. Sci. U. S. A.* **116**, 20366-20375 (2019).
606 34. Netzker, T., et al. An efficient method to generate gene deletion mutants of the rapamycin-
607 producing bacterium *Streptomyces iranensis* HM 35. *Appl. Environ. Microbiol.* **82**, 3481-3492 (2016).
608 35. Gerlitz, M., Hammann, P., Thiericke, R. & Rohr, J. The biogenetic origin of the carbon skeleton
609 and the oxygen atoms of elaiophylin, a symmetric macrodiolide antibiotic. *J. Org. Chem.* **57**, 4030-
610 4033 (1992).
611 36. Haydock, S., Mironenko, T., Ghoorahoo, H. & Leadlay, P. The putative elaiophylin biosynthetic
612 gene cluster in *Streptomyces* sp. DSM4137 is adjacent to genes encoding adenosylcobalamin-
613 dependent methylmalonyl CoA mutase and to genes for synthesis of cobalamin. *J. Biotechnol.* **113**,
614 55-68 (2004).
615 37. Zhou, Y., Prediger, P., Dias, L., Murphy, A. & Leadlay, P. Macrodiolide formation by the
616 thioesterase of a modular polyketide synthase. *Angew. Chem. Int. Ed.* **54**, 5232-5235 (2015).
617 38. Du, L. & Lou, L. PKS and NRPS release mechanisms. *Nat. Prod. Rep.* **27**, 255-278 (2009).
618 39. Kautsar, S., Blin, K., Shaw, S., Weber, T. & Medema, M. BiG-FAM: the biosynthetic gene cluster

619 families database. *Nucleic Acids Res.* **49**, D490-D497 (2021).
620 40. Navarro-Munoz, J., et al. A computational framework to explore large-scale biosynthetic diversity.
621 *Nat. Chem. Biol.* **16**, 60-68 (2020).
622 41. Komaki, H. Resolution of housekeeping gene sequences used in MLSA for the genus *Streptomyces*
623 and reclassification of *Streptomyces anthocyanicus* and *Streptomyces tricolor* as heterotypic synonyms
624 of *Streptomyces violaceoruber*. *Int. J. Syst. Evol. Microbiol.* **72**, 005370 (2022).
625 42. Coban, O., De Deyn, G. & van der Ploeg, M. Soil microbiota as game-changers in restoration of
626 degraded lands. *Science* **375**, eabe0725 (2022).
627 43. De Souza, R., Ambrosini, A. & Passaglia, L. M. P. Plant growth-promoting bacteria as inoculants
628 in agricultural soils. *Genet. Mol. Biol.* **38**, 401-419 (2015).
629 44. Lopes, M., Dias, M. & Gurgel, E. Successful plant growth-promoting microbes: inoculation
630 methods and abiotic factors. *Front. sustain. food syst.* **5**, 606454 (2021).
631 45. Zhu, J. Salt and drought stress signal transduction in plants. *Annu. Rev. Plant Biol.* **53**, 247-273
632 (2002).
633 46. Maurel, C., et al. Aquaporins in plants. *Physiol. Rev.* **95**, 1321-1358 (2015)
634 47. Kaldenhoff, R. & Fischer, M. Functional aquaporin diversity in plants. *Biochim. Biophys. Acta*
635 *Biomembr.* **1758**, 1134-1141 (2006).
636 48. Shi, H., Ishitani, M., Kim, C. & Zhu, J. The *Arabidopsis thaliana* salt tolerance gene SOS1 encodes
637 a putative Na^+/H^+ antiporter. *Proc. Natl. Acad. Sci. U. S. A.* **97**, 6896-6901 (2000).
638 49. Ji, H., et al. The Salt Overly Sensitive (SOS) pathway: established and emerging roles. *Mol. Plant*
639 **6**, 275-286 (2013).
640 50. Shi, H., Lee, B., Wu, S. & Zhu, J. Overexpression of a plasma membrane Na^+/H^+ antiporter gene
641 improves salt tolerance in *Arabidopsis thaliana*. *Nat. Biotechnol.* **21**, 81-85 (2003).
642 51. McDonald, B. & Currie, C. Lateral gene transfer dynamics in the ancient bacterial genus
643 *Streptomyces*. *Mbio* **8**, e00644-17 (2017).
644 52. Chase, A., Sweeney, D., Muskat, M., Guillen-Matus, D. & Jensen, P. Vertical inheritance facilitates
645 interspecies diversification in biosynthetic gene clusters and specialized metabolites. *Mbio* **12**, e02700-
646 21 (2021).
647 53. Vergnes, S., et al. Phyllosphere colonization by a soil *Streptomyces* sp. promotes plant defense
648 responses against fungal infection. *Mol. Plant-Microbe Interact.* **33**, 223-234 (2020).
649 54. Li, X., Tian, Y., Peng, H., He, B. & Gao, K. Isolation, screening and identification of an antagonistic
650 actinomycetes to control *Fusarium* wilt of *Momordica charantia*. *Ying Yong Sheng Tai Xue Bao* **31**,
651 3869-3879 (2020).
652 55. Yun, T., et al. Anti-Foc RT4 activity of a newly isolated *Streptomyces* sp. 5-10 from a medicinal

plant (*Curculigo capitulate*). *Front. Microbiol.* **11**, 610698 (2021).

56. Chung, Y., et al. Comparative genomics reveals a remarkable biosynthetic potential of the *Streptomyces* phylogenetic lineage associated with rugose-ornamented spores. *Msystems* **6**, e00489-21 (2021).

57. Jiang, M., et al. GdmRIII, a TetR family transcriptional regulator, controls geldanamycin and elaiophylin biosynthesis in *Streptomyces autolyticus* CGMCC0516. *Sci. Rep.* **7**, 4803 (2017).

58. He, W., et al. Crossregulation of rapamycin and elaiophylin biosynthesis by RapH in *Streptomyces rapamycinicus*. *Appl. Microbiol. Biotechnol.* **106**, 2147-2159 (2022).

59. Raaijmakers, J. & Kiers, E. Rewilding plant microbiomes. *Science* **378**, 599-600 (2022).

60. Tsugawa, H., et al. MS-DIAL: data-independent MS/MS deconvolution for comprehensive metabolome analysis. *Nat. Methods* **12**, 523-526 (2015).

61. Madeira, F., et al. Search and sequence analysis tools services from EMBL-EBI in 2022. *Nucleic Acids Res.* **50**, W276-W279 (2022).

62. Letunic, I. & Bork, P. Interactive Tree Of Life (iTOL) v5: an online tool for phylogenetic tree display and annotation. *Nucleic Acids Res.* **49**, W293-W296 (2021).

Acknowledgements

We acknowledge Dr. Yaojun Tong for the discussions on CRISPR-BEST. We thank the support from Dr. Charlotte Held Gotfredsen (DTU NMR Centre), and Dr. Aaron John Christian Andersen (DTU Metabolomics Core). We acknowledge financial support from Carlsberg Infrastructure (CF20-0177), Novo Nordisk Foundation Proof of Concept (NNF20OC0062267), DTU Enable Program, InnoExplorer Grant, Innovation Fund Denmark, and Danish National Research Foundation (DNRF137) for support towards the Centre for Microbial Secondary Metabolites (CeMiSt). Z.Y. acknowledges funding from the China Scholarship Council (202004910340). T.W. acknowledges funding from the Novo Nordisk Foundation (NNF20CC0035580).

Author contributions

Z.Y. and T.W. designed and carried out genetic experiments and bioinformatic analyses. E.S. isolated the metabolites and characterised the structures; L.D. did structure elucidation, compounds crystalision, and preliminary plant assays; Z.Y., Y.Q., N.C.K. and E.A. performed the plant and qRT-PCR assays; G. P. and M. A. carried out large scale fermentation and downstream processing; P.H. carried out X-ray crystallography and data analysis. All the authors discussed the results and commented on the manuscript.

Competing interests

685 The authors declare no competing interests.

686

687 **Correspondence** and requests for materials should be addressed to Ling Ding.

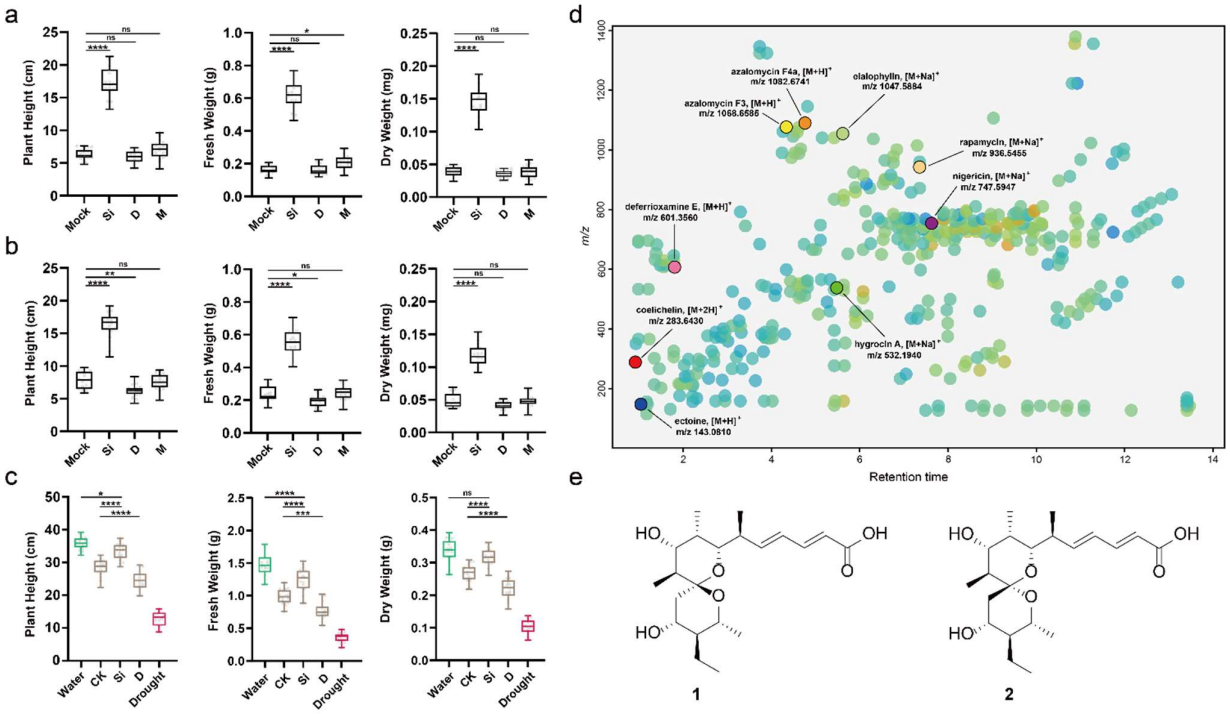

Fig. 1. The effect of *S. iranensis* on barley seedlings under the abiotic stress and the bioactive components produced by *S. iranensis*. ***a***, the box plots (middle bar=median, box limit=upper and lower quartile, extremes=min and max values) depict the plant height, fresh weight and dry weight of barley seedlings growing under osmotic stress mediated by 20% (w/v) PEG-6000 (*n*=18). Abbreviation: ***Mock***, control; ***Si***, treatment of *S. iranensis* culture broth; ***D***, treatment of *S. iranensis*/Δ*ptaA* culture broth; ***M***, treatment of blank medium (ISP2); Statistical significance was assessed by one-way ANOVA with post hoc Dunnett's multiple comparisons test. ***b***, the box plots depict the plant height, fresh weight and dry weight of barley seedlings growing under salinity stress mediated by 100 mM NaCl (*n*=18). Abbreviation: ***Mock***, control; ***Si***, treatment of *S. iranensis* culture broth; ***D***, treatment of *S. iranensis*/Δ*ptaA* culture broth; ***M***, treatment of blank medium (ISP2). Statistical significance was assessed by one-way ANOVA with post hoc Dunnett's multiple comparisons test. ***c***, the box plots depict the plant height, fresh weight and dry weight of barley seedlings growing under drought stress (*n*=18). Different colours of box plots indicate different growing conditions: green, 21 days water; brown, 7 days treatment after 7 days water followed by 7 days drought; red, 7 days water followed by 14 days drought. Statistical significance was assessed by one-way ANOVA with Tukey test. Abbreviation: ***Water***, well water for 21 days; ***CK***, 7 days treatment of water after 7 days water + 7 days drought; ***Si***, 7 days treatment of *S. iranensis* culture broth after 7 days water + 7 days drought; ***D***, 7 days treatment of *S. iranensis*/Δ*ptaA* culture broth after 7 days water + 7 days drought; ***M***, treatment of blank medium (ISP2); ***Drought***, 14 days drought after 7 days water. Statistical significance was assessed by one-way ANOVA with Tukey test. ***d***, the metabolite profile of the native *S. iranensis* growing in liquid ISP2 medium, the known secondary metabolites were identified by HR-LC-MS/MS and highlighted; ***e***, the bioactive components pteridic acid H (**1**) and pteridic acid F (**2**) isolated from *S. iranensis*.

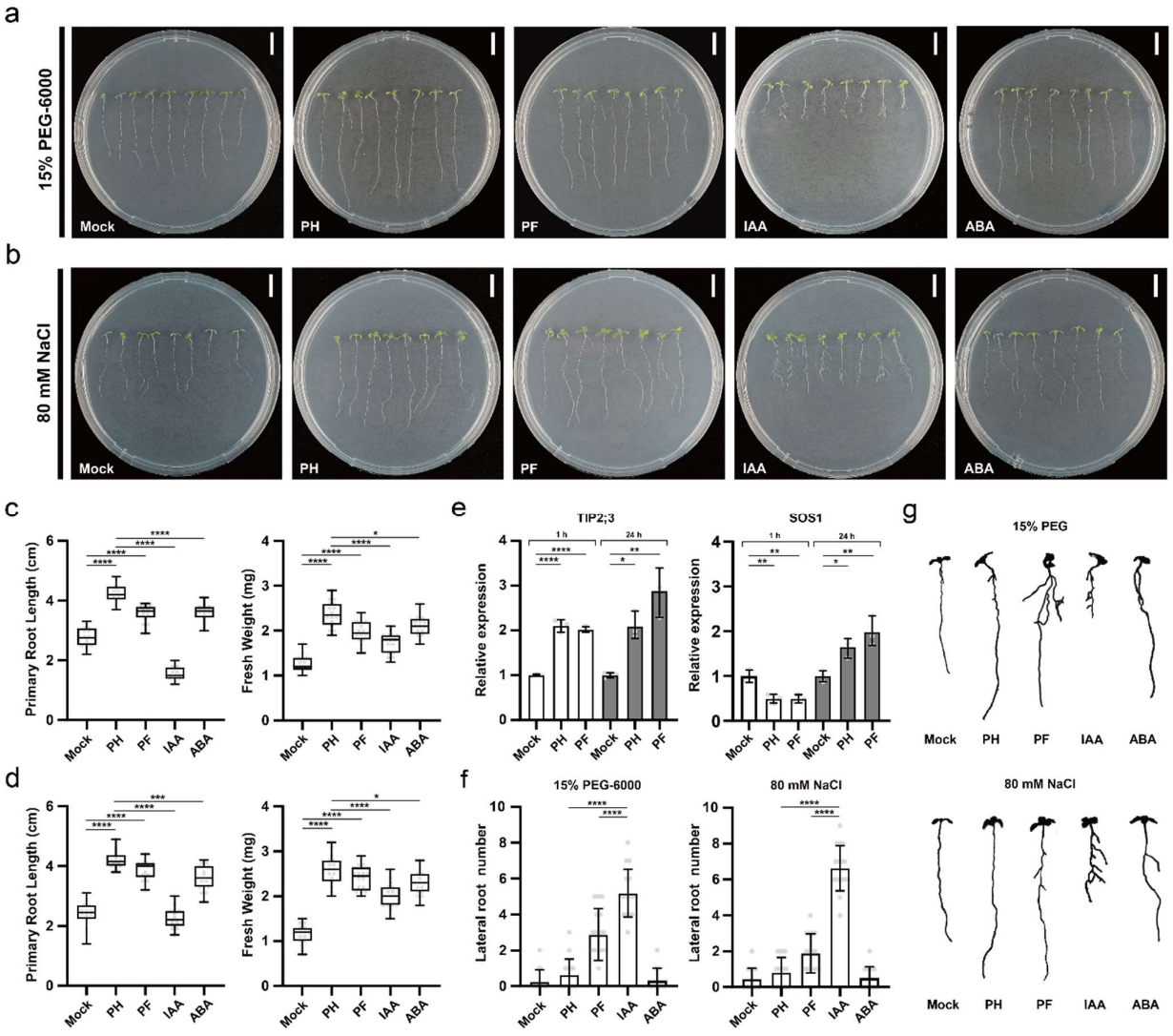

Fig. 2. The effect of pteridic acids H and F on *Arabidopsis* seedlings under abiotic stress. ***a***, phenotype of *Arabidopsis* seedlings growing under drought stress mediated by 15% (w/v) PEG-6000 using other treatments (bars=1 cm); ***b***, phenotype of *Arabidopsis* seedlings growing under salinity stress mediated by 80 mM NaCl using other treatments (bars=1 cm); ***c***, the box plots (middle bar=median, box limit=upper and lower quartile, extremes=min and max values) depict the primary root length and fresh weight of *Arabidopsis* seedlings growing on non-stress condition (n=16). Statistical significance was assessed by one-way ANOVA with Tukey test; ***d***, the box plots depict the primary root length and fresh weight of *Arabidopsis* seedlings growing on drought stress condition (n=16). Statistical significance was assessed by one-way ANOVA with Tukey test; ***e***, the relative expression level of TIP2;3 and SOS1 in *Arabidopsis* seedlings under salinity stress were measured after 1 hour and 24 hours of different treatments. Each treatment contains three biological replicates. Statistical significance was assessed by one-way ANOVA with post hoc Dunnett's multiple comparisons test; ***f***, the lateral root number of *Arabidopsis* seedlings growing in different conditions (n=16). Statistical significance was assessed by one-way ANOVA with post hoc Dunnett's multiple comparisons test. ***g***, the phenotype differences of lateral root growth of *Arabidopsis* seedlings growing in other conditions. Abbreviations: ***Mock***, control; ***PH***, treatment of 0.5 ng mL^{-1} pteridic acid H; ***PF***, treatment of 0.5 ng mL^{-1} pteridic acid F; **IAA**, treatment of 1.3 nM indole-3-acetic acid; ***ABA***, treatment of 1.3 nM abscisic acid.

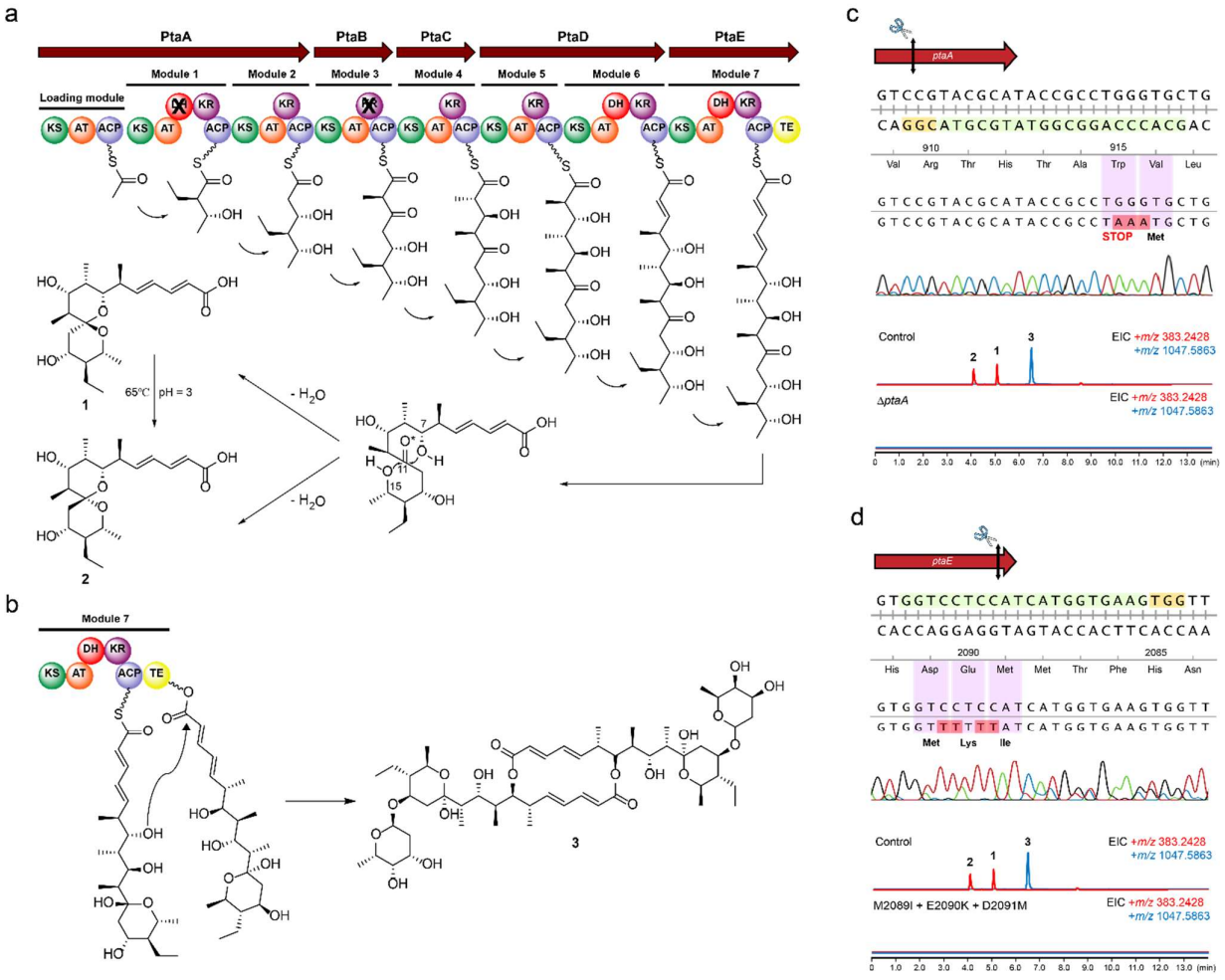

725

726 **Fig. 3**. Biosynthesis mechanism of pteridic acids and CRISPR base editing application in *S. iranensis*. ***a***, the proposed
727 biosynthetic pathway of pteridic acids H (**1**) and F (**2**); ***b***, the proposed biosynthesis mechanism of elaiophylin (**3**),
728 and its macrodiolide formation is catalysed by thioesterase (TE) domain. ***c***, Sanger sequencing and LC-MS/MS
729 output of CRISPR base editing application of STOP codon introduction targeting the *ptaA* of *S. iranensis*. The 20-nt
730 protospacer sequence is highlighted in light green, whereas the 3-nt PAM sequence is shown in yellow. The codons
731 and corresponding amino acids are indicated, and the black double-headed arrow represents the position of the editing
732 window; ***c***, Extracted Ion Chromatography (EIC) for **1** and **2** (*m/z* 383.2428 $[M+H]^+$) and **3** (*m/z* 1047.5863 $[M+Na]^+$)
733 in the wild type *S. iranensis* (Control) and the mutant *S. iranensis*/Δ*ptaA*; ***d***, Sanger sequencing and LC-MS/MS
734 output of CRISPR base editing application of site-directed mutagenesis targeting the TE domain of *pta* BGC. EIC
735 for **1** an **2** (*m/z* 383.2428 $[M+H]^+$) and **3** (*m/z* 1047.5863 $[M+Na]^+$) in the wild type *S. iranensis* (Control) and the
736 mutant *S. iranensis*/M2089I + E2090K + D2091M.

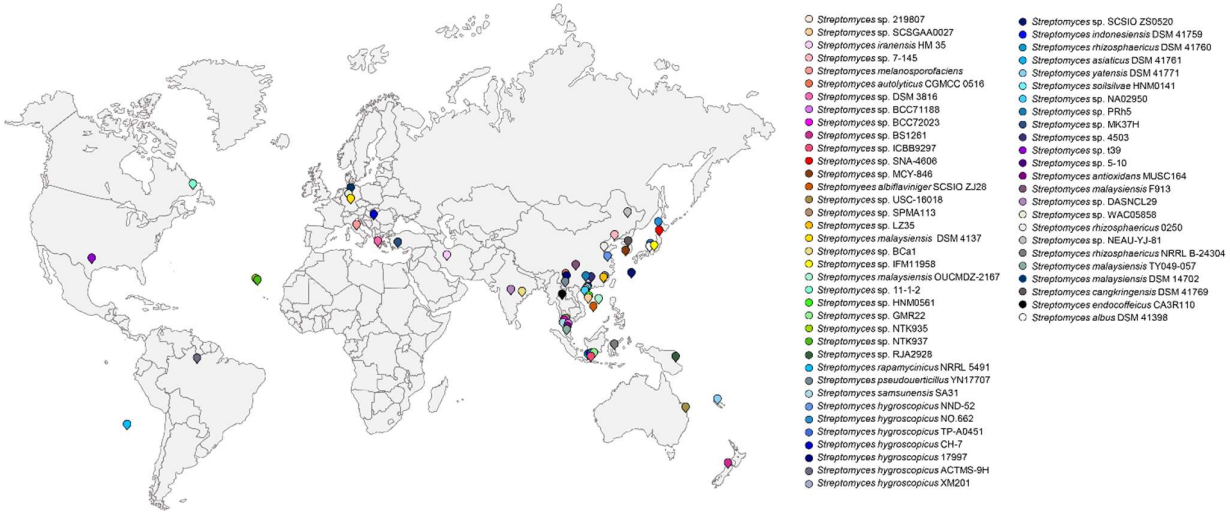

737

738 **Fig. 4.** Geographical distribution of *pta*-containing *Streptomyces* strains possessing *pta* BGC. A total of 62
739 *Streptomyces* strains were displayed on the map and distinguished by different colours. For detailed strain information,
740 see Supplementary Tab. 4.

741

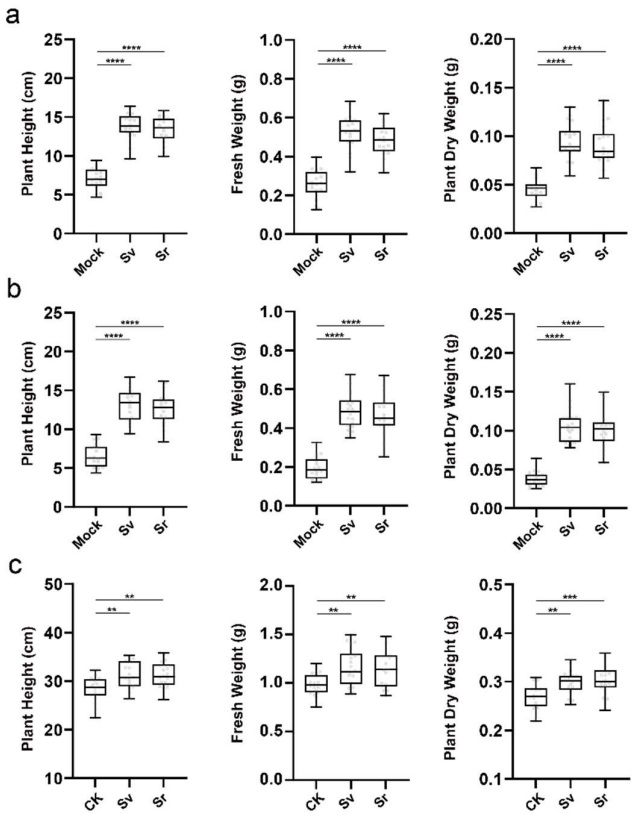

Fig. 5. Abiotic stresses alleviation led by *S. violaceusniger* Tu 4113 and *S. rapamycinicus* NRRL 5491. ***a***, the box plots (middle bar=median, box limit=upper and lower quartile, extremes=min and max values) shows different growth of barley seedlings in osmotic stress mediated by 20% (w/v) PEG-6000 (n=16). Abbreviation: ***Mock***, control; ***Sv***, treatment of *S. violaceusniger* Tu 4113 culture broth; ***Sr***, treatment of *S. rapamycinicus* NRRL 5491 culture broth; ***b***, different growth of barley seedlings in salinity stress mediated by 100 mM NaCl (n=16). Abbreviation: ***Mock***, control; ***Sv***, treatment of *S. violaceusniger* Tu 4113 culture broth; ***Sr***, treatment of *S. rapamycinicus* NRRL 5491 culture broth; ***c***, different growth of barley seedlings in drought stress (n=16). Abbreviation: ***CK***, 7 days treatment of water after 7 days water + 7 days drought; ***Sv***, 7 days treatment of *S. violaceusniger* Tu 4113 culture broth after 7 days water + 7 days drought; ***Sr***, 7 days treatment of *S. rapamycinicus* NRRL 5491 culture broth after 7 days water + 7 days drought. Statistical significance was assessed by one-way ANOVA with post hoc Dunnett's multiple comparisons test.

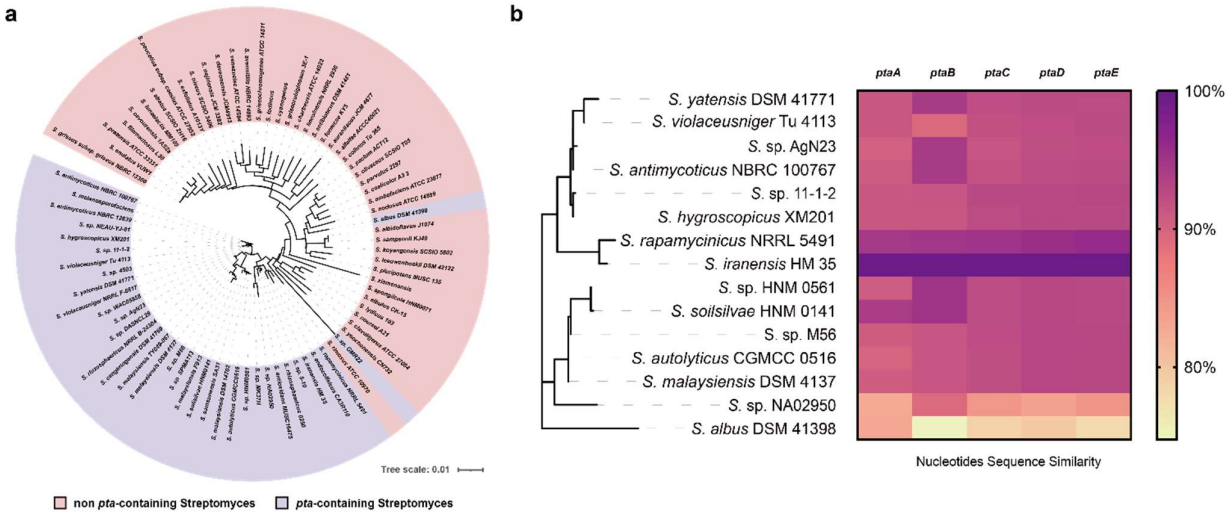

Fig. 6. The phylogenetic and secondary metabolites BGCs analysis of *pta*-containing *Streptomyces* strains. ***a***, the phylogenetic tree of 16S rRNA nucleotides sequences of *pta*-containing *Streptomyces* and other *Streptomyces* strains; ***b***, the heatmap depicts similarity differences of core biosynthetic genes of *pta* BGC between *S. iranensis* and other 14 *pta*-containing *Streptomyces* strains.